

Crystal Phase Control During Epitaxial Hybridization of III-V Semiconductors with Silicon

Marta Rio Calvo, Jean-Baptiste Rodriguez, Charles Cornet, Laurent Cerutti, Michel Ramonda, Achim Trampert, Gilles Patriarche and Éric Tournié**

Dr. M. Rio Calvo, Dr. J.-B. Rodriguez, Dr. L. Cerutti, Pr. É. Tournié
IES, University of Montpellier, CNRS, F- 34000 Montpellier, France
E-mail: jean-baptiste.rodriguez@umontpellier.fr, eric.tournie@umontpellier.fr

Pr. C. Cornet
Univ Rennes, INSA Rennes, CNRS, Institut FOTON – UMR 6082, F-35000 Rennes, France

Dr. M. Ramonda
CTM, University of Montpellier, F- 34000 Montpellier, France

Dr. A. Trampert
Paul-Drude-Institut für Festkörperelektronik, Leibniz-Institut im Forschungsverbund Berlin e.V., Hausvogteiplatz 5-7, 10117, Berlin, Germany

Dr. G. Patriarche
Université Paris-Saclay, CNRS, Centre de Nanosciences et de Nanotechnologies, 91120, Palaiseau, France

Keywords: epitaxial growth, anti-phase domains, monolithic integration, III-V semiconductors, silicon substrates

Abstract

The formation and propagation of anti-phase boundaries (APBs) in the epitaxial growth of III-V semiconductors on Silicon is still the subject of great debate, despite the impressive number of studies focusing on this topic in the last past decades. The control of the layer phase is of major importance for the future realization of photonic integrated circuits that include efficient light sources or for new nano-electronic devices, for example. Here, we experimentally demonstrate that the main-phase domain overgrows the anti-phase domains (APDs) because it grows faster. A large-scale analysis of the phase evolution based on reflection high-energy electron diffraction and atomic force microscopy in the case of the molecular beam epitaxy of GaSb on Silicon (001) substrate is presented. The growth rate difference between the two domains is accurately measured and is shown to come from the atomic step distribution at the III-V surface. The influence of the substrate preparation as well as of the growth condition on this distribution is also clarified.

1. Introduction

Silicon, an earth-abundant material (27.7% of the earth crust), exhibits an unmatched combination of economic, electronic, mechanical and thermal properties that has revolutionized the 20th Century through the development of the microelectronics industry and the emergence of information and communication technologies (ICTs) at large. This industry has proved very successful in guiding the microelectronic ecosystem to synchronize the technological progress and manufacturing techniques with societal needs through the implementation of ever-shrinking technology nodes, in line with the Moore's Law. The "More Moore" approach continues this trend toward increasing performances by applying new transistor concepts and/or incorporating new materials into devices. As the 21st Century dawned however, the massive data traffic demand of our hyper-connected society as well as the need for non-digital functions (e.g., RF communication, power control, passive components, sensors, actuators) to interact with the outside world called for new strategies known as "More-than-Moore".^[1] Ubiquitous to both "More-Moore" and "More-than-Moore" technologies is the hybridization of different materials with Silicon-based platforms.

Among "More-than-Moore" strategies, the integration of optical devices with Silicon has attracted much attention. Indeed, the development of efficient light-emitting, energy-harvesting, or light-engineering systems on silicon not only holds several advantages for the development of today's technologies (e.g. silicon photonics,^[2-4] photovoltaics,^[5] or sensors^[6-7]) but it could also open novel paradigms in photonics, computing or energy harvesting and storage applications (e.g. integrated quantum photonics,^[8] all-optical neuromorphic computing,^[9] or solar water splitting.^[10] Silicon is however not naturally suitable for most optical applications, as it has an indirect band structure.^[3] While its low optical absorption can be somewhat counterbalanced by using thick absorbers – the strategy followed in conventional solar cells – its low radiative efficiency fundamentally limits its use for the development of light

emitters, especially lasers.^[11–15] Thus, the hybridization of Silicon with other optical materials such as perovskites^[10] or organic materials^[16] was seriously considered in the recent years.

In this context, III-V semiconductors remain the optical materials of choice, as they combine excellent optical properties (with direct bandgaps for most of them), device and bandgap engineering capabilities through alloying, doping and heterostructure design, robustness and stability of the devices, and mature processing technologies developed for years in various optoelectronic applications. While the most advanced demonstrations of III-V/Si hybrid photonic systems were obtained by bonding chips, devices or wafers,^[6–7] the monolithic integration, where the III-V crystal is directly grown on the Si substrate is considered as the long-term solution.^[17] Equally important, III-V semiconductors exhibit excellent transport properties which put them at the core of the “More-Moore” developments.^[1] All these strategies however require the silicon wafer to be nominally oriented – i.e. the miscut angle should not be higher than 0.5° – to be compatible with the microelectronics industry.^[18]

The epitaxial hybridization of III-V devices on Si has long been hampered by the high density of defects generated during the growth.^[19,20] One of the issues to be solved arises from the fact that Si has a non-polar diamond crystal structure, whereas most III-V materials have a polar zinc-blende crystal structure (except nitrides with a wurtzite structure).^[21] As a result, the epitaxial growth of III-V semiconductors on Si substrates allows the simultaneous formation of two different III-V crystal phases, or polar-domains.^[22] Wherever two domains of different polarities intersect, a two-dimensional defect is generated. These so-called anti-phase boundaries (APBs) consist of III-III and/or V-V bonds,^[23,24] resulting locally in an excess or a lack of charges, and in a significant modification of the electronic band structure and vibrational properties.^[25,26] Threading APBs are therefore a critical issue as far as they introduce efficient vertical electrical path within the III-V heterostructure, thereby killing the performances of any p-n junction device.^[25,27] Engineering the APBs generation and propagation at the early stages of the III-V growth on Si is thus the only way to fully benefit from the ultimate properties of

integrated III-V semiconductors and a major prerequisite for the successful monolithic integration of III-V optoelectronic devices on Si photonic platforms^[28,29] or III-V/Si energy harvesting devices.^[5]

In 1987, Kroemer^[30] gave a first description of APBs generation, correlating the domain distribution and the local step structure of the initial Si surface. Theoretically, a Si surface only populated with biatomic steps does not allow the formation of APBs, as long as the III-V layer growth is uniformly initiated with the same group atoms (i.e. forming either III-Si bonds or V-Si bonds) and provided that the abrupt-interface atomic structure is strictly preserved during the first monoatomic layer deposition, without intermixing. Accordingly, the generation of the two III-V variants was ascribed to the presence of the mono-atomic steps often found on on-axis Si surfaces.^[31] The most widespread strategy to avoid APBs has thus consisted in using Si substrates with an off-cut of 4 to 6° towards the [110] direction, in order to enhance the density of stable biatomic steps.^[32] However, these substrates are not compatible with the silicon industry standards, which rely on “on-axis” Si substrates with an off-cut tolerance around 0.5°. A great deal of effort has therefore been devoted to promote a double-step organization of “on-axis” Si surfaces through specific surface preparation. This approach has proved particularly effective in a metal-organic chemical vapor deposition (MOCVD) environment.^[33–36] Advanced Si preparation strategies have also been proposed recently including the implementation of V-groove patterned Si substrates,^[37] template-assisted selective epitaxy,^[38, 39] and III–V nano-ridge engineering.^[40] Although successful at preventing the propagation and, to a lesser extent, the generation of APBs, these techniques however rely on complex processing and patterning of the Si surface prior to the growth.

Regarding the growth on planar substrates, it was occasionally demonstrated back in the 80s that APBs could self-annihilate within the III-V layer, eventually leading to a decrease of the density of APBs emerging at the III-V surface.^[35,41–45] Although several studies have later corroborated these observations,^[46–48] the process behind the annihilation mechanism

remains unclear. In 1987, Kawbe et al. proposed the existence of two types of APBs: APBs that run perpendicular to the interface and propagate through the whole III-V layer, and APBs that run on tilted planes and self-annihilate during growth.^[41,49] It was widely assumed that the stoichiometric $\{110\}$ APBs, that run perpendicular to the interface, are the more common.^[49-51] Therefore, in order to reduce the number of emerging APBs, some studies aimed at promoting the generation of tilted APBs.^[35] Moreover, in 2020, K. Li et al.^[48] indicated a correlation between the organization of the Si surface and the APBs annihilation. They observed that a non-organized Si substrate leads to random APBs nucleation which leads to emerging APBs. In contrast, a well-organized single-stepped Si substrate leads to the nucleation of a periodic array of APBs that later tilt and annihilate during the growth. They, however, did not suggest any explanation for this behavior.

Recently, a different description of the growth of III-V semiconductors on Si(001) emerged in the literature, which we briefly summarize in the following. Due to energetic considerations, it was demonstrated that III-V semiconductors always nucleate as three-dimensional islands, having their own polarity independently of the underlying Si-step structure.^[52] As a consequence, APBs are created during the hetero-phase coalescence of islands having different polarities. The growth then proceeds and a progressive transition to a two-dimensional layer is generally observed. With this picture in mind, the so-called APBs annihilation was further described as the result of the overgrowth by one polar-domain, the main-phase-domain (MPD), of the other domain, the anti-phase domain (APD),^[53] suggesting by itself that the process is more an APD burying, than the result of APB self-annihilation. This overgrowth mechanism is thought to arise from the fact that : i) a III-V surface can exhibit two kinds of steps, namely III- and V- steps,^[54] ii) the group-III atoms incorporation rate at the step edges depends on the type of steps,^[55,56] and iii) on a regularly stepped III-V surface, i.e. on a surface where all the steps follow the same direction, the two domains will have different types of steps: if the MPD is populated with III-steps, then the APD only exhibits V-steps at the

surface, and vice-versa. Incorporation rates at III- and V- steps also depend on the growth conditions used through the temperature and V/III ratio. In this model, group-III adatoms diffuse on the III-V surface and eventually incorporate at steps, with a higher incorporation probability on the phase having the more favorable step configuration. The steps within the MPD, therefore propagate faster than the APD steps, which results in the burying of the APD. Interestingly, this model does not involve any consideration on the APB propagation planes but instead implies that the efficacy of the APD burying is primarily bound to the existence of a regularly-stepped III-V surface. To be fulfilled, this condition requires on the one hand a uniform initial step direction distribution at the Si surface, obtained through a careful choice of the residual miscut angle and a specific substrate preparation, and, on the other hand, on a step-flow growth mode of the III-V material to preserve the initial step distribution. Although supported by some indirect observations and theoretical calculations,^[53] this model however still lacks of a clear experimental demonstration.

In this work, we combined reflection high-energy electron diffraction (RHEED), transmission electron microscopy (TEM) and atomic-force microscopy (AFM) to analyze the structural and surface properties of GaSb layers grown on Si(001) substrates by Molecular Beam Epitaxy (MBE). We experimentally demonstrate that the APD burying process is a consequence of the growth rate imbalance. We also show that the APD burying can be achieved on Si(001) substrates having a small off-cut angle towards [110], a crucial step for the development of high-quality monolithically hybridized III-V/Si devices with applications in photonics, energy harvesting or microelectronics. **The growth conditions of the GaSb layers presented in this paper are summarized in the Supporting Information, and more details can be found in reference [57].**

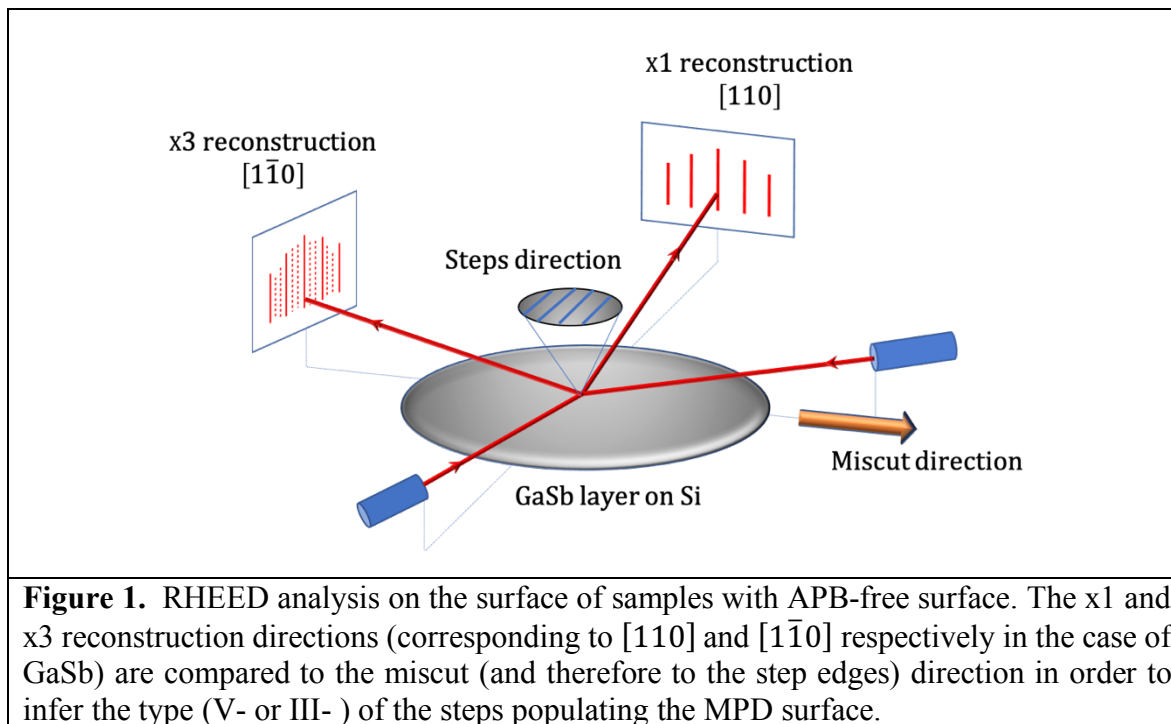
2. Large scale analysis of the phase distribution evolution

The growth was monitored through in situ RHEED, which confirmed that the initial Si surface exhibited a superposition of (1x2) and (2x1) reconstructions, indicating the presence of steps having a height corresponding to an odd number of Si monolayers (mono-atomic steps for instance).^[22] From that perspective, the annihilation of the APBs using our growth technique can hardly be ascribed to the presence of a large density of stable biatomic steps, in sharp contrast with the experiments conducted by MOVPE described above.^[33-36] RHEED observations also revealed that the GaSb growth consistently starts with the formation of 3D islands. After coalescence of the GaSb islands and transition to a 2D layer growth mode, the RHEED pattern indicated a superposition of (1x3) and (3x1) surface reconstructions. **The GaSb reconstruction under the typical growth conditions used here being a (1x3), this demonstrates the presence of APDs. The (3x1) reconstruction was found to vanish as the GaSb thickness increased, which is consistent with the burying of the APDs confirmed by cross-section TEM (Figure S1) and AFM measurements.** RHEED is therefore a powerful technique that allows assessing in situ and in “real-time” the presence of the two domains on a relatively large area. In particular, it allows assessing which of the two initial phases becomes the MPD. The two domains are indeed equivalent, the only difference being that the [110] direction of one domain corresponds to the $[1\bar{1}0]$ direction of the other. This distinction made between these two directions is relevant for the III-V layer but is of course meaningless for the Si substrate due to its diamond structure. Identifying the main crystallographic directions of the final III-V layer (by TEM for example), and comparing them to that of the substrate therefore does not help in answering the question regarding which phase finally transformed into the MPD. We propose that the only way to solve this problem is to identify the type of step populating the MPD, which can be done using RHEED once the APBs have been successfully removed from the surface. To that end, we compared the miscut direction to the x1 and x3 reconstructions (**Figure 1**). The

miscut direction is indeed perpendicular to the step edge lines in a properly prepared sample, and therefore, it can be easily concluded that V-steps (resp. III-steps) are populating the MPD if the x_3 (resp. x_1) reconstruction is found parallel to the miscut direction (because on one hand, the x_1 and x_3 reconstruction directions give access to the $[110]$ and $[1\bar{1}0]$ directions respectively, and on the other hand, a step edge lying on a x_1 (resp. x_3) direction is necessarily a V-step (resp. a III-step)). This analysis was repeated on several samples and we systematically found the situation schematized on Figure 1 where the MPD is populated by V-steps. None of the growth conditions explored in this work resulted in an MPD having III-steps, which could be due to the fact that MBE inherently favors V-steps when the growth is conducted in excess of element V flux, which was always the case in this study. This again highlights the role of the miscut, extensively discussed in reference,^[53] which could be summarized in the fact that it serves as a mechanism used to suppress the additional degree of symmetry found in the Diamond structure with respect to the Zinc-Blende. In other words, the miscut imposes a single step direction (this again requires a proper preparation of the Si surface and a III-V step-flow growth mode), and the growth method/conditions can then be tuned to favor one type of steps, resulting in the burying of the domain populated by the “wrong” type.

RHEED however results in a qualitative analysis, and in order to get a more quantitative picture of the burying process, the samples were thoroughly characterized by atomic force microscopy (AFM). Transmission electron microscopy (TEM) was also conducted on some selected samples as a complementary technique to validate the identification of the APBs derived from AFM. To illustrate this, we show in **Figure 2** AFM and TEM results obtained on the same GaSb/Si sample. Deep dark regions having unpredictable shapes and being randomly distributed can be seen on the topographic image (Figure 2(a)). Figure 2(b) shows a cross-section dark field (DF)-TEM image of the same sample, where diffraction contrast related to the presence of APBs threading from the interface all the way up to the surface of the III-V layer is clearly visible. High-angle annular dark-field (HAADF) scanning TEM (STEM) also

confirmed the different crystal polarity on each side of the APB (Figure 2(c)), by directly imaging the atomic columns with chemically-sensitive contrast.



The different polarities can directly be seen by observing the Ga-Sb dumbbells in each domain (insets in Figure 1 (c)). In addition, cross-section TEM images show that the GaSb thickness is significantly smaller (about 20 nm in the case shown in Figure 2(b)) in the APD. This thickness difference was observed on several samples, which clearly confirmed that the deep dark regions seen on the AFM scans coincide with the areas where APDs emerge at the sample surface.

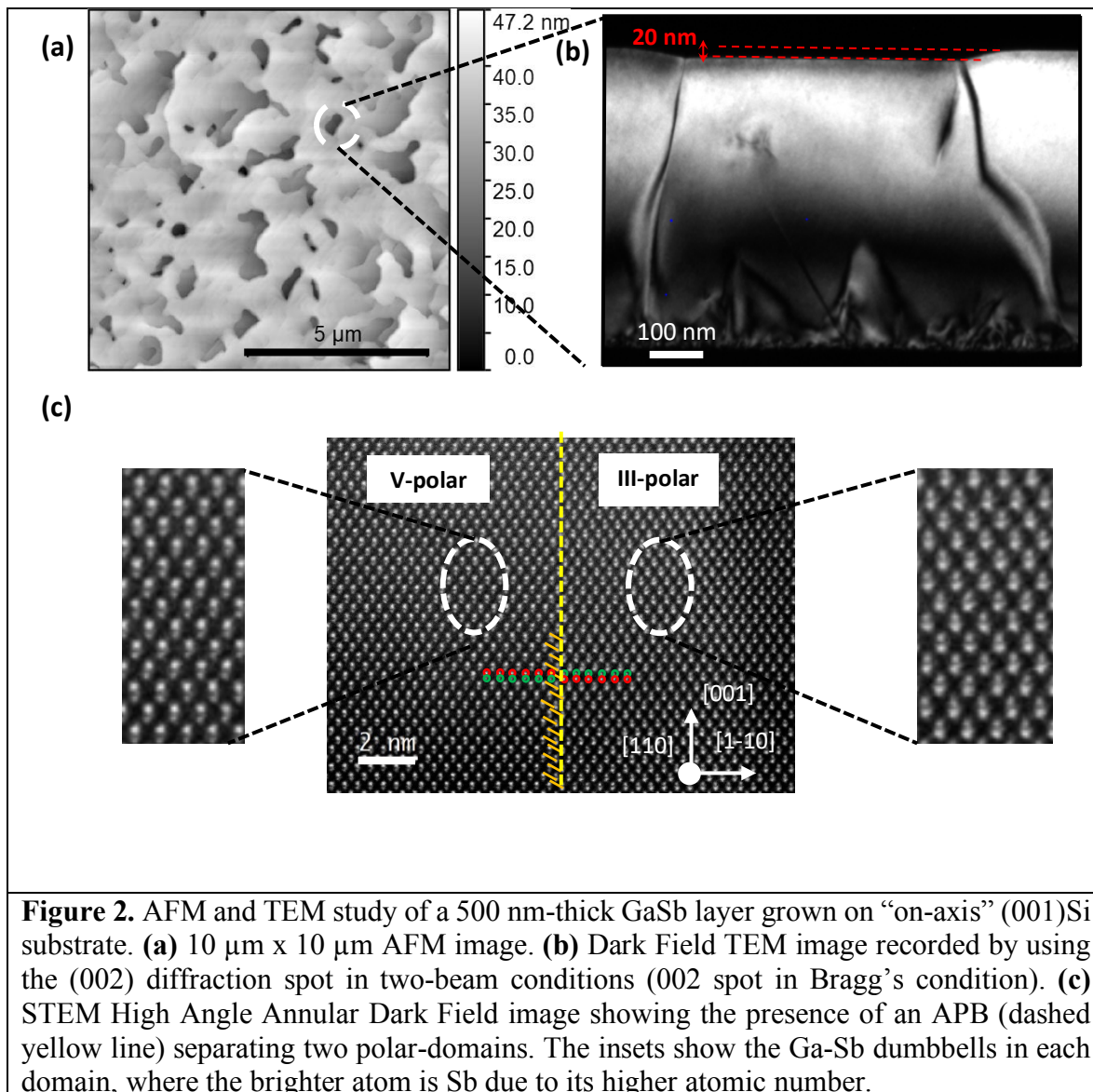


Figure 2. AFM and TEM study of a 500 nm-thick GaSb layer grown on “on-axis” (001)Si substrate. **(a)** 10 μm x 10 μm AFM image. **(b)** Dark Field TEM image recorded by using the (002) diffraction spot in two-beam conditions (002 spot in Bragg’s condition). **(c)** STEM High Angle Annular Dark Field image showing the presence of an APB (dashed yellow line) separating two polar-domains. The insets show the Ga-Sb dumbbells in each domain, where the brighter atom is Sb due to its higher atomic number.

A more detailed analysis of the AFM images was then carried out using the Gwyddion software,^[58] and the methodology is illustrated in **Figure 3**. First, the identification of the two crystal polarities was performed by adjusting an abrupt threshold to the height distribution, as shown in inset of Figure 3. This allowed to extract the percentage of the surface covered by emerging APDs (hereafter referred as APD surface coverage), as well as the density of emerging APBs obtained by dividing the total APBs length by the total area of the AFM image. The height distribution for the whole scanned area was then extracted and adjusted using a two-Gaussian peak fitting, and the peak at the lowest height was ascribed to the APDs. In the

example shown in Figure 3, the two domains clearly have different mean heights, and subtracting the mean height of the APD to that of the MPD thus gives direct access to the average thickness difference of the GaSb layer between the two domains. This analysis is therefore particularly efficient at giving a statistical overview of the thickness difference existing between the two domains, as a large sample area spanning over several dozens of APDs is analyzed within a single AFM image. The example in Figure 3 shows a 500 nm-thick GaSb layer having an emerging APB density of $0.6 \mu\text{m}^{-1}$. The APDs cover 7.5% of the sample surface, and are on average 12 nm-thinner than the MPDs.

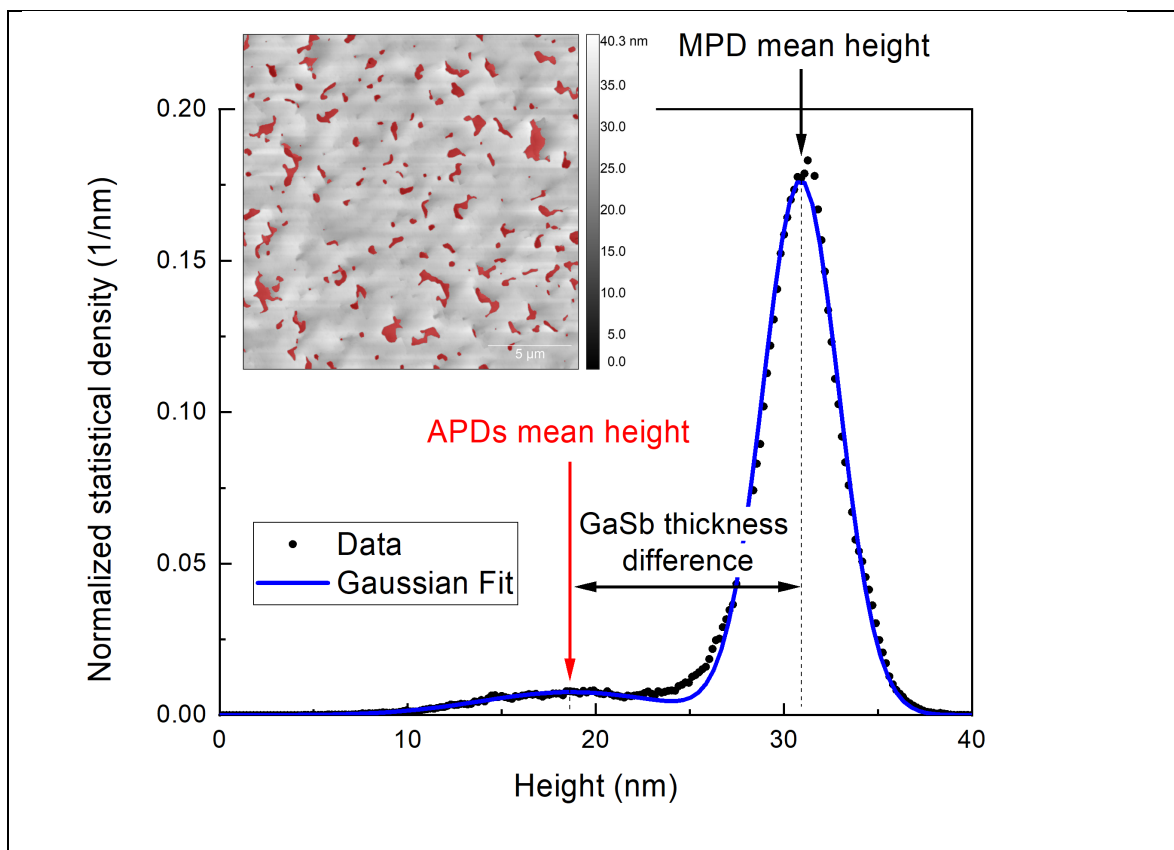


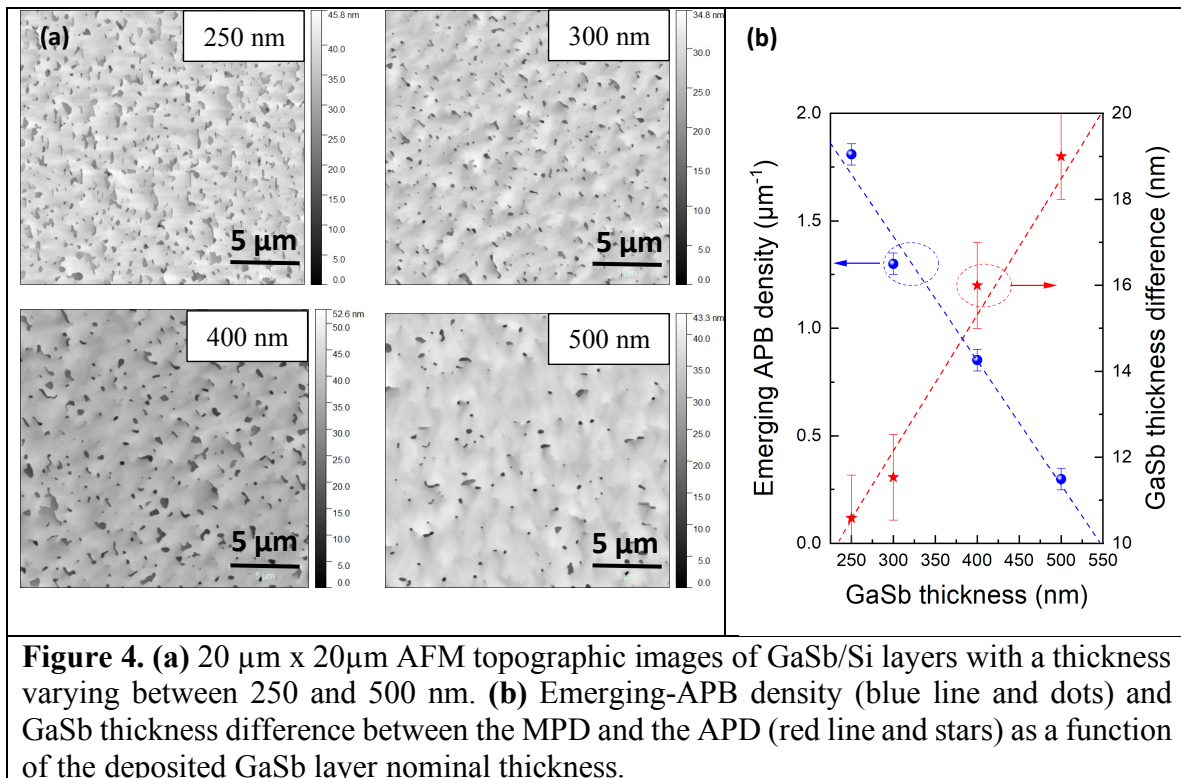
Figure 3. Height profile (black dots) extracted from the $20 \times 20 \mu\text{m}^2$ AFM topographic image shown in inset (the APDs have been masked in red using an abrupt threshold applied on the height value). The x-axis of the profile corresponds to the depth scale of the AFM image, where $x = 0$ represents the deepest region. Two Gaussian peaks were used to fit the data (blue line), and the maximum intensity of each peak was ascribed to the mean height of a phase domain. The separation between the two peaks gives access to the mean GaSb thickness difference between the two domains, which is about 12 nm in this example.

3. Analysis of the APD Burying Process

3.1. Determination of the Growth-Rate Difference Between the Two Polar-Domains

Within the burying model framework,^[53] one of the main conditions to promote the MPD overgrowth, and hence the annihilation of the APBs, is that one polar-domain grows faster than the other one. In the following, we evidence and quantify the growth rate difference between the two polar-domains during III-V/Si hetero-epitaxy.

A set of four GaSb samples grown on Si(001) substrates having an off-cut of 0.5° towards the [110] direction was studied. All the samples were grown using the very same conditions (cf. section Methods), apart from the GaSb layer nominal thickness, which was varied between 250 and 500 nm.



From the analysis of the surface morphology of these samples measured by AFM (**Figure 4**), some important results were obtained: First, the density of emerging APBs was found to decrease as the GaSb layer thickness increases (Figure 4 (b)), which confirms the

progressive nature of the burying process, already suggested by the RHEED observations described above. A linear fit of the evolution of the emerging APBs density with the GaSb thickness allows determining that, on average, the emerging APB density decreases at a rate of $0.0057 \mu\text{m}^{-1}$ per nanometer of deposited GaSb. The extrapolation of this fit suggests that under these growth conditions a thickness of about 550 nm would be necessary to totally suppress emerging APBs from the GaSb surface. Additionally, the phase domain covering the smallest surface, always appear in Figure 4 (a) as darker regions, indicating that the GaSb layer is always thinner within the APD than within the MPD. The method described in Figure 3 was used to analyze the variation of the thickness difference between the two polar-domains as a function of the GaSb nominal thickness (Figure 4 (b)). The thickness difference increases with the nominal thickness, which unambiguously demonstrates that the MPD and the APD have different growth rates and confirms the central assumption of the burying model presented in reference [53] and summarized in the introduction. Besides, the linear dependence indicates that the growth rate difference remains constant over the thickness range studied here. The slope of the linear fit of the data points in Figure 3 (b) thus allows quantifying the growth rate difference (Δgr), using the following expression:

$$\frac{dD}{dt} = \frac{gr_{MPD} - gr_{APD}}{gr} \quad (1)$$

Where D is the thickness difference, t the GaSb nominal thickness, gr_{MPD} , gr_{APD} , and gr are the growth rates of the MPD, the APD and the nominal growth rate respectively.

The slope of the linear curve is therefore equal to $\Delta gr / gr$, which results in a growth rate relative difference of about 3%, or 0.0096 ML.s^{-1} considering the nominal growth rate of 0.3 ML.s^{-1} . From this analysis, and assuming that gr_{MPD} is equal to the nominal growth rate (i.e. the growth rates of the MPD and the APD are 0.3 and ML.s^{-1} , respectively), one can determine the growth rate imbalance coefficient ($C_{APD/MPD}$), defined in reference [53] as the ratio between

the growth rates of the APD and the MPD (but never measured directly), which is equal to 0.968 in the present growth conditions.

In summary, we have demonstrated that it indeed exists a growth rate difference between the two domains, which is the central assumption of the burying model. Thanks to a large-scale analysis based on AFM measurements, we were able to accurately determine this growth rate difference in the case of the growth of GaSb on Si (001) substrates. The values found are however believed to be dependent on many parameters, which we examine in more detail in the following paragraphs.

3.2. Importance of the III-V Steps Organization

The previous section established that the growth rate difference of the two polar-domains found within a GaSb layer grown on a Si surface is the fundamental mechanism enabling the burying of the APD. The burying model described in ref [53] ascribes this mechanism to a proper organization of the III-V steps towards a single and same direction throughout the two polar-domains. To clarify the influence of the organization of the III-V steps on the APD annihilation process, we analyzed topographic AFM images of 500 nm-thick GaSb layers grown using optimized and non-optimized substrate preparations. **The optimized preparation is detailed in the Supporting Information, and consists, in short, in an ex-situ cleaning followed by an in-situ high-temperature annealing. For the non-optimized sample, the high-temperature annealing was omitted, which is expected to have a great impact on the step ordering at the Si surface.** Figure 5 (a) and (b) show the AFM images of the non-optimized sample in which the GaSb step-flow can be seen both along and perpendicular to the [110] direction within each polar-domain. As schematically represented in Figure 5 (c), in this case, the Si off-cut was clearly not correctly transferred everywhere to the GaSb step organization. A large density of APBs of about $2 \mu\text{m}^{-1}$ was observed in this topographic AFM image and the

APDs cover nearly half the total area. Figure 5 (d) and (e) show the AFM images recorded with the optimized sample in which it appears that both polar-domains are populated with steps following the same $[110]$ direction (Figure 5 (f)).

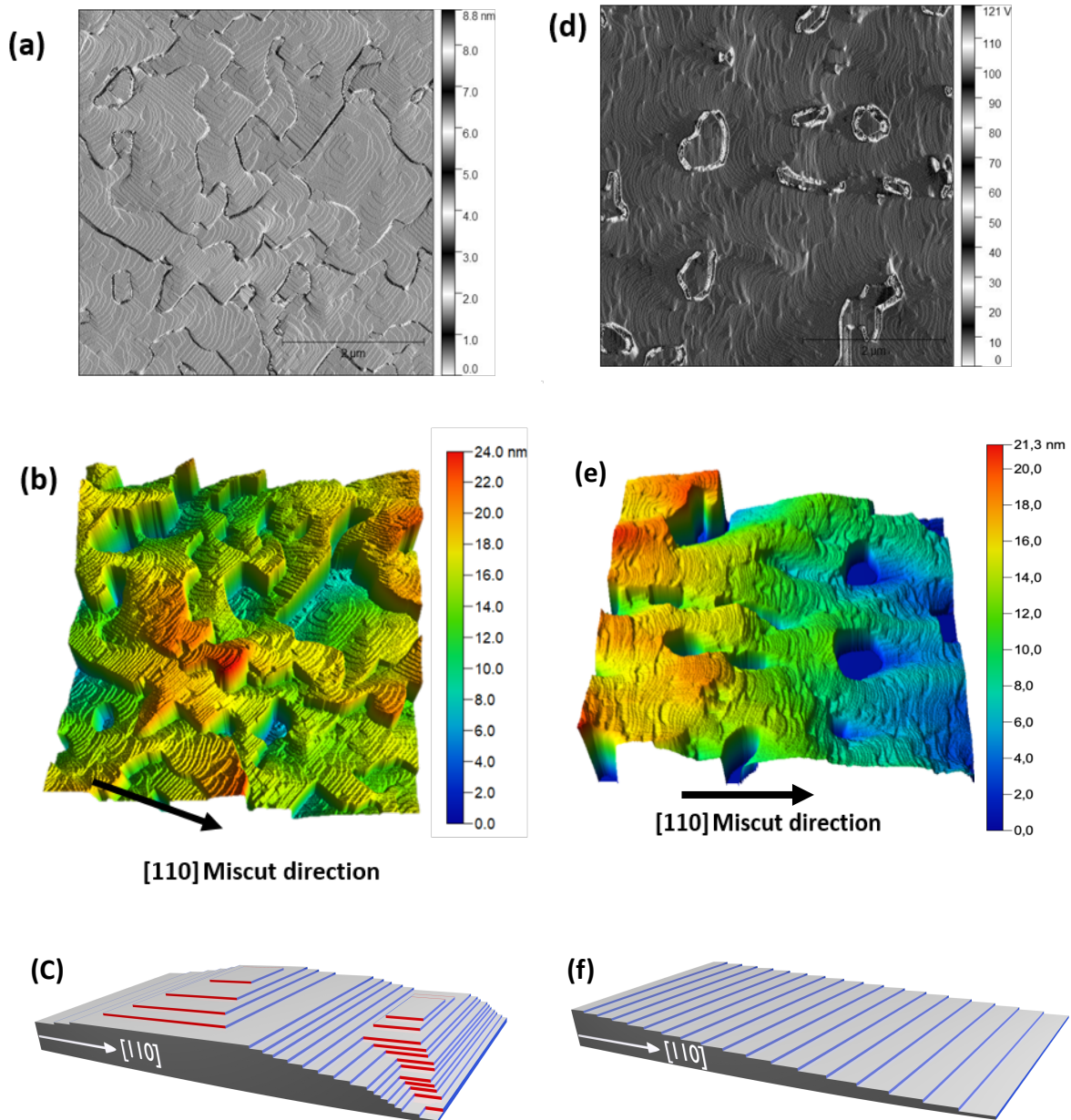


Figure 5 . 5 μm x 5 μm AFM image, the corresponding 3D AFM image and the sketch of a 500 nm-thick GaSb layer deposited on 0.5° Si (001) substrate prepared under non-optimized ((a), (b), (c)), and optimized ((d), (e), (f)) conditions.

In this case, the sample presented a significantly lower density of emerging APBs of only $0.2 \mu\text{m}^{-1}$. Although not being a quantitative demonstration, this result clearly supports the claim that the APB density is largely influenced by the distribution of the steps direction among the two domains. According to the burying model interpretation, in the first case, (Figure 5 (a) and (b)), both domains grow on average at the same rate because the two polar-domains have, statistically, the same number of III- and V-steps, and therefore, none of the polar-domain can overgrow the other one. By contrast, in the second case (Figure 5 (d) and (e)), the well-organized III-V stepped surface promotes a predominant density of one type of step in each of the two polar-domains, which triggers the growth rate difference of the two domains, due to the incorporation rate difference existing between III- and V- steps. This result also highlights the central role of the sample preparation as it allows the formation of steps having a single direction throughout the whole Si surface. Beyond the preparation technique, the substrate offcut is another parameter influencing the steps distribution, which is discussed in the next section.

3.3. Influence of the Substrate Off-Cut Angle

The proper choice of the Si substrate off-cut angle value and direction is essential to achieve APD burying and thus APB annihilation during the III-V growth.^[53,59] This section focuses on the experimental study of the influence of the off-cut angle on the APD burying process. For this purpose, a set of GaSb layers grown on Si (001) substrates with different off-cut angles (0.18° , 0.5° , and 1°) towards the $[110]$ direction and different GaSb layer thicknesses was prepared using the growth conditions presented in the Method section. Whatever the miscut angle, we consistently observed the same steady decrease of the APD density with the increase of the GaSb thickness already described above in the case of the 0.5° off-cut. For each off-cut angle value however, the GaSb thickness required to completely remove the APBs from the

sample surface (determined from the evolution of the APD density with the layer thickness, similar to the method presented in Figure 4) was different (Figure 6). It clearly appears from this experiment that the smaller the Si off-cut angle, the thicker the GaSb layer must be to completely bury the APDs, in the off-cut range under study. In fact, the off-cut value was found to have a dramatic impact on the burying process: only about 200 nm of GaSb has to be grown to obtain APB-free samples for an off-cut of 1° , when it is more than $1.2 \mu\text{m}$ for an off-cut of 0.18° . The impact is also more severe as the angle value decreases, which is consistent with the fact that for an ideal substrate with no off-cut (perfectly oriented Si (001)), there would be no more driving force organizing the steps direction, resulting in a situation where the APBs could not be removed anymore, whatever the GaSb thickness.

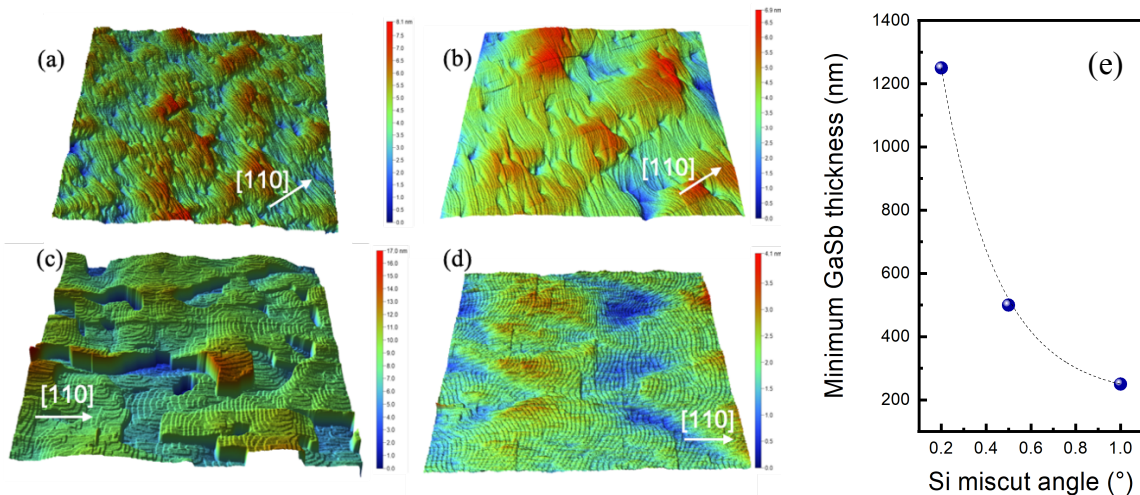


Figure 6. 3D $5 \times 5 \mu\text{m}$ AFM images of 500 nm-thick GaSb layers deposited on (a) 1° , (b) 0.5° and (c) 0.18° miscut Si substrates. (d) $1.5 \mu\text{m}$ -thick GaSb layer deposited on a 0.18° miscut Si substrate. (e) Minimum layer thickness required to completely annihilate the emerging-APBs as a function of the Si off-cut angle.

To better understand this observation, we compare in the following the topographic AFM images measured on the 500 nm-thick GaSb layers deposited on the three different off-cut Si substrates (Figure 6 (a), (b) and (c)). The GaSb layers grown on 1° and 0.5° off-cut Si substrates reveal a mono-domain surface, whereas the sample grown on 0.18° off-cut Si exhibits emerging APBs. The two samples having a mono-domain surface (Figure 6 (a), (b)), present a

proper organization of the GaSb steps in a single direction, consistent with the off-cut direction. In contrast, steps in both the direction parallel and perpendicular to the off-cut direction can be seen at the surface of the sample with emerging-APBs (Figure 6 (c)). Still, a careful analysis of Figure 6 (c) confirms that if the two polar-domains grow with both types of steps, a higher density of steps is found towards the [110] direction. This inhomogeneous distribution of the step direction certainly explains why emerging APBs can eventually be removed, even at low off-cut angles (0.18°), although at the price of a thicker GaSb layer, as shown on Figure 6 (d). This clearly contrasts with the situation described earlier (Figure 5 (a)) where a nearly equal density of steps could be found in both directions, due to an improper surface preparation. In this case, increasing the GaSb thickness indeed did not result in a decrease of the APB density, which further emphasizes the strong relationship between the domain growth rate difference and the asymmetrical initial distribution of the steps direction.

Interestingly, the burying model^[53] does not predict any variation of the growth rate difference with the off-cut angle used, as long as this angle is large enough to ensure a sufficient step-flow growth mode (estimated to 0.03° toward a [110] direction). This conclusion was drawn considering that the miscut is perfectly transferred to both MPD and APD, thus leading to a perfectly regular lattice of III-steps and V-steps at the III-V surface, in the different domains, respectively. In this situation, for a given miscut the density of steps would always be the same in both domains, thus leading to a constant growth rate imbalance coefficient, whatever the off-cut angle. The observation of the steps at the III-V surfaces provided by 3D AFM images in Figure 5 and 6 clearly demonstrates that this is an idealized picture, as a too low substrate off-cut angle or a Si surface preparation of a lesser quality can both result to a situation where both III-steps and V-steps coexist within a same domain, with a significant impact on the growth rate imbalance.

We therefore ascribe the result of Figure 5 to the fact that : (i) the widening of the (001) terraces at smaller off-cut implies that higher energy must be provided to perfectly organize the

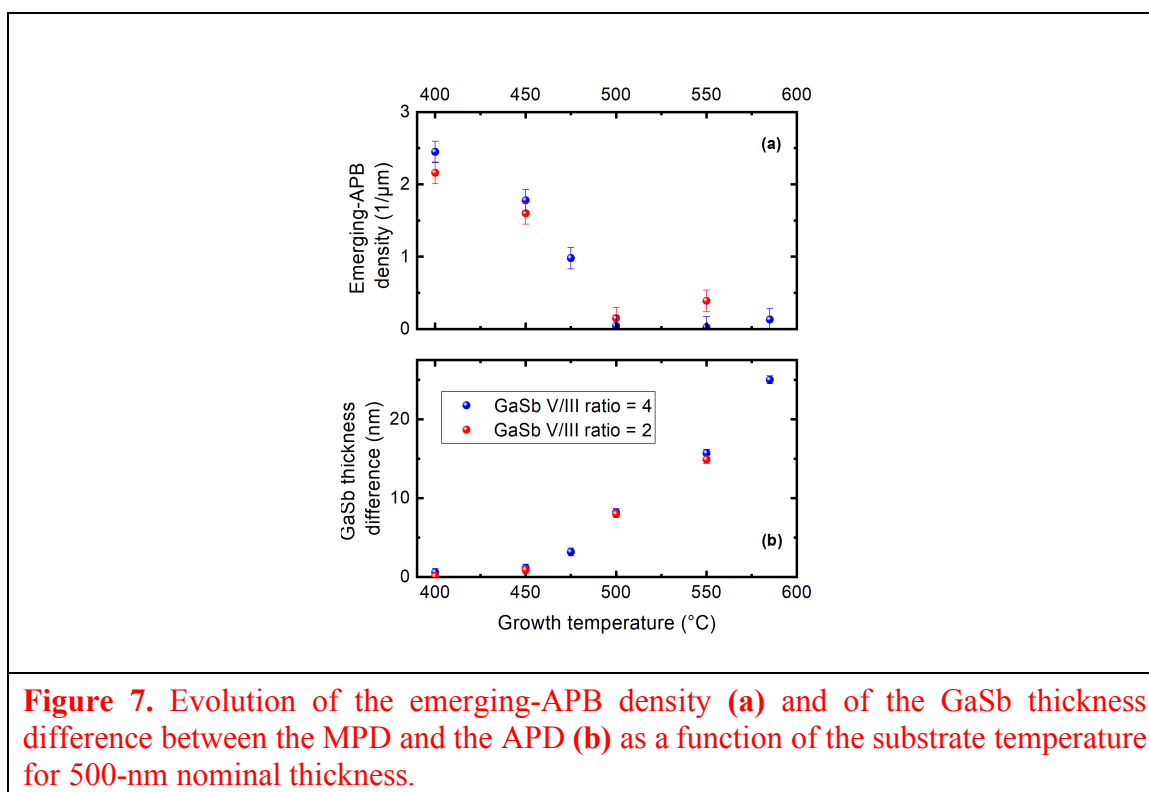
surface as step-edges are moved apart and interact less, and (ii) the transfer of the off-cut direction to the III-V step direction distribution is disrupted at small off-cut by the influence of the local Si roughness and by the overall substrate bowing, which also relate to both the substrate preparation and the substrate heater and holder geometries. Nevertheless, we experimentally confirmed in this section that APD burying can be achieved even for very low miscut angles ($<0.2^\circ$), provided the off-cut angle and direction are well controlled, and a high-quality silicon substrate preparation is applied prior to the growth.

3.4. In Situ Crystal Phase Control

The III-V growth conditions were found to have a fundamental role in the burying of APDs.^[35,60] In the general framework of the burying model,^[53] two physical parameters have been predicted to significantly impact the steps incorporation rates, and thus the growth rate imbalance coefficient: the V/III ratio and the substrate temperature. In this section, we focus on the influence of these two parameters on the APD burying process in the case of GaSb layers grown on 0.5° Si (001) substrates. Two sets of samples were grown with substrate temperatures in the 400 to 600°C range for the growth of the high-temperature GaSb layer at two different V/III maximum incorporation rate ratios of 2 and 4. The substrate preparation and growth conditions for the low-temperature GaSb layer were kept the same for the whole set (cf. section Method). Figure 7 (a) shows the variation of the mean thickness difference between the MPD and the APD as a function of the substrate growth temperature and the GaSb V/III ratio. Figure 7 (b) shows the corresponding density of emerging-APBs.

No significant variation of the mean thickness difference between the two polar-domains was observed when changing the V/III ratio between 2 and 4. In contrast, the burying process was found to be strongly influenced by the growth temperature. At low substrate temperature (below 450°C), a large density of APBs (in the 1.5 to $2.5 \mu\text{m}^{-1}$ range) emerges and

the thickness difference between the two polar-domains is close to none, which indicates a very slow APD overgrowth process if any. Above 450°C, however, the thickness difference increases, and the APB density decreases significantly and monotonically with increasing temperatures. It is worth mentioning that the best APB density obtained among these 500 nm-thick GaSb layers is as low as $0.01 \mu\text{m}^{-1}$, which is much better than previous reports for GaSb ($0.53 \mu\text{m}^{-1}$ for a 1 μm -thick GaSb layer^[61]) and is comparable to the best results for GaAs ($0.01 \mu\text{m}^{-1}$ for a 600 nm-thick GaAs layer^[35]). We note here that for such a low value, it becomes difficult to statistically evaluate the density of emerging APBs, and the surface thus exhibits a near-to-ideal monodomain configuration. We recently used samples grown in a similar way on 2-inch on-axis Si(001) as templates for the successful growth of laser diodes emitting at 2.3 μm as well as of InAs/AlSb based quantum-cascade lasers.^[47,62]



The strong correlation between the substrate growth temperature and the surface APDs disappearance rate indicates that the burying of the APDs is a thermally-activated process. At low substrate temperatures, we ascribe the ineffective burying process to the fact that the growth conditions do not enable the step-flow growth mode required for triggering the growth rate difference between the two domains. Above 450°C, the step-flow is significant/established and the enhancement of the annihilation rate with temperature depends on the variation of the incorporation rates at III- and V- steps^[53] as well as, although probably to a lesser extent, on the increase of the Ga atom diffusion length at the GaSb surface. The growth temperature is the most important parameter to control (promote or hamper) the APB burying process in the specific case of the GaSb/Si MBE growth within the usual experimental conditions (400-550°C range, V/III ratio between 2 and 4). Nevertheless, incorporation rates on V- or III- steps strongly depend on the chemical elements considered and on the growth technique. To determine the precise influence of the physical III-V growth parameters on the growth rate imbalance, a similar study should be conducted for each specific III-V semiconducting material, and for each growth technique used.

4. Conclusion

In summary, we have studied the APB annihilation process in the case of the MBE growth of GaSb layers on Si (001) substrates having small off-cut angles in the [110] direction. In good agreement with the recently proposed burying mechanism, we demonstrated that the APD is overgrown by the MDP. The overgrowth occurs through a growth rate difference of the two polar-domains, that we were able to quantify. This growth rate difference was found to be relatively small, about 3% of the nominal growth rate, but allows completely suppressing the APBs from the surface of a 500 nm-thick GaSb layer grown on an 0.5° off-cut Si (001) substrate. The efficacy of this overgrowth mechanism was found to strongly depend on the off-cut angle.

It was observed that smaller off-cut angles result in an incomplete transfer of the miscut to the III-V steps direction distribution, which in turns decreases the growth rate difference due to the concomitant presence of both III- and V- steps at the surface of each polar-domain. In the worst-case scenario, where the Si substrate was not properly prepared, the off-cut could not act as a driving force to dictate the steps direction, which resulted in the total absence of annihilation. Finally, the influence of the growth conditions was clarified: while the V/III ratio was found to have nearly no influence, the substrate temperature proved to have a dramatic impact on the burying efficacy.

This study represents the first experimental clarification of the burying mechanism governing the APBs annihilation in III-V layers grown by MBE on Si (001) substrates having small off-cut angles. Interestingly, this interpretation can also explain the recent results of Li et al. who observed in the growth of GaAs on Si that a perfect organization of the Si surface (although not necessarily a bi-stepped surface) was mandatory to avoid APBs emerging at the surface.^[48] Other III-V-on-Si materials systems and other growth techniques should now be studied in a similar way to extend our findings and establish generic rules for possible enhancement of the growth rate difference for example. **Although it was developed to be valid for any III-V, we note that in the theoretical model of the burying mechanism presented in reference [53], the “case study” is GaAs and not GaSb. It would thus be rather surprising that it only applies to GaSb, although experimental evidence with other materials are still missing at this point.** The better comprehension of these mechanisms will be the key towards a reduction of the APB density that will enable the hybridization of high-performance III-V devices with industry-compatible Si substrates.

Acknowledgements

Part of the work has been supported by the French program on Investment for the Future (ANR-11-EQPX-0016) and the H2020 program of the European Union (GA 780240). This work received support from the Renatech network for part of the transmission electron microscopy studies. AT acknowledges the support within the frame of the European Regional Development Fund (ERDF), project number 2016011843.

Conflict of Interest

The authors declare no conflict of interest.

References

- [1] W. Arden, M. Brillouët, P. Coge, M. Graef, B. Huizing, and R. Mahnkopf, “More-than-Moore’ White Paper,” <https://go.nature.com/2BAMo7L> (ITRS, **2010**).
- [2] R. Soref and J. Lorenzo, “All-silicon active and passive guided-wave components for $\lambda = 1.3$ and $1.6 \mu\text{m}$,” *IEEE J. Quantum Electron.*, vol. 22, no. 6, pp. 873–879, Jun. **1986**, doi: 10.1109/JQE.1986.1073057.
- [3] W. N. Ye and Y. Xiong, “Review of silicon photonics: history and recent advances,” *J. Mod. Opt.*, vol. 60, no. 16, pp. 1299–1320, Sep. **2013**, doi: 10.1080/09500340.2013.839836.
- [4] D. A. B. Miller, “Attojoule Optoelectronics for Low-Energy Information Processing and Communications,” *J. Light. Technol.*, vol. 35, no. 3, pp. 346–396, Feb. **2017**, doi: 10.1109/JLT.2017.2647779.
- [5] Markus Feifel, David Lackner, Jonas Schön, Jens Ohlmann, Jan Benick, Gerald Siefer, Felix Predan, Martin Hermle and Frank Dimroth, “Epitaxial GaInP/GaAs/Si Triple-Junction Solar Cell with 25.9% AM1.5g Efficiency Enabled by Transparent Metamorphic $\text{Al}_x\text{Ga}_{1-x}\text{As}_y\text{P}_{1-y}$ Step-Graded Buffer Structures”, *Solar RRL*, p. 2000763, mars **2021**, doi:10.1002/solr.202000763
- [6] R. Helkey, A. A. M. Saleh, J. Buckwalter and J. E. Bowers, “High-Performance Photonic Integrated Circuits on Silicon,” *IEEE J. Sel. Top. Quantum Electron.*, vol. 25, no. 5, pp. 1–15, Sep. **2019**, doi: 10.1109/JSTQE.2019.2903775.
- [7] Chennupati Jagadish, Sebastian Lourdudoss and John E. Bowers “Future Directions in Silicon Photonics, Volume 101 - 1st Edition.”, Elsevier Accessed: Sep. 15, **2020**. <https://www.elsevier.com/books/future-directions-in-silicon-photonics/jagadish/978-0-12-818857-6>.

- [8] J. Wang, F. Sciarrino, A. Laing and M. G. Thompson “Integrated photonic quantum technologies” *Nature Photonics* volume 14, pages273–284 (2020), doi:[10.1038/s41566-019-0532-1](https://doi.org/10.1038/s41566-019-0532-1)
- [9] J. Feldmann, N. Youngblood, C. D. Wright, H. Bhaskaran and W. H. P. Pernice “All-optical spiking neurosynaptic networks with self-learning capabilities” *Nature* **569**, 208–214 (2019). doi:[10.1038/s41586-019-1157-8](https://doi.org/10.1038/s41586-019-1157-8)
- [10] Siva Krishna Karuturi, Heping Shen, Astha Sharma, Fiona J. Beck, Purushothaman Varadhan, The Duong, Parvathala Reddy Narangari, Doudou Zhang, Yimao Wan, Jr-Hau He, Hark Hoe Tan, Chennupati Jagadish and Kylie Catchpole, “Over 17% Efficiency Stand-Alone Solar Water Splitting Enabled by Perovskite-Silicon Tandem Absorbers” *Advanced energy materials* Volume10, Issue28 (2020), doi:[10.1002/aenm.202000772](https://doi.org/10.1002/aenm.202000772)
- [11] B. Jalali and S. Fathpour, “Silicon Photonics,” *J. Light. Technol.*, vol. 24, no. 12, pp. 4600–4615, Dec. 2006, doi: 10.1109/JLT.2006.885782.
- [12] Haisheng Rong, Richard Jones, Ansheng Liu, Oded Cohen, Dani Hak, Alexander Fang and Mario Paniccia, “A continuous-wave Raman silicon laser,” *Nature*, vol. 433, no. 7027, pp. 725–728, Feb. 2005, doi: 10.1038/nature03346.
- [13] Zhizhong Yuan, Aleksei Anopchenko, Nicola Daldosso, Romain Guider, Daniel Navarro-Urrios, Alessandro Pitanti, Rita Spano, and Lorenzo Pavesi, “Silicon Nanocrystals as an Enabling Material for Silicon Photonics” *Proc. IEEE*, vol. 97, no. 7, pp. 1250–1268, Jul. 2009, doi: 10.1109/JPROC.2009.2015060.
- [14] John Rönn, Weiwei Zhang, Anton Autere, Xavier Leroux, Lasse Pakarinen, Carlos Alonso-Ramos, Antti Säynätjoki, Harri Lipsanen, Laurent Vivien, Eric Cassan and Zhipei Sun, “Ultra-high on-chip optical gain in erbium-based hybrid slot waveguides,” *Nat. Commun.*, vol. 10, no. 1, p. 432, Dec. 2019, doi: 10.1038/s41467-019-08369-w.
- [15] H. Ye and J. Yu, “Germanium epitaxy on silicon,” *Sci. Technol. Adv. Mater.*, vol. 15, no. 2, p. 024601, Apr. 2014, doi: 10.1088/1468-6996/15/2/024601.

- [16] Sebastian Koeber, Robert Palmer, Matthias Lauermann, Wolfgang Heni, Delwin L Elder, Dietmar Korn, Markus Woessner, Luca Alloatti, Swen Koenig, Philipp C Schindler, Hui Yu, Wim Bogaerts, Larry R Dalton, Wolfgang Freude, Juerg Leuthold and Christian Koos “Femtojoule electro-optic modulation using a silicon–organic hybrid device” *Light Sci Appl* **4**, e255 (2015), doi:10.1038/lssa.2015.28
- [17] J.-S. Park, M. Tang, S. Chen, and H. Liu, “Heteroepitaxial Growth of III-V Semiconductors on Silicon,” *Crystals*, vol. 10, no. 12, Art. no. 12, Dec. 2020, doi: 10.3390/cryst10121163.
- [18] Charles Cornet Yoan Léger Cédric Robert, “Integrated Lasers on Silicon - 1st Edition.” <https://www.elsevier.com/books/integrated-lasers-on-silicon/cornet/978-1-78548-062-1> (accessed Jun. 27, 2021).
- [19] D. B. Holt and B. G. Yacobi, “Extended Defects in Semiconductors”, doi.org/10.1017/CBO9780511534850 (accessed Apr. 30, 2020).
- [20] B. Kunert, Y. Mols, M. Baryshniskova, N. Waldron, A. Schulze, and R. Langer, “How to control defect formation in monolithic III/V hetero-epitaxy on (100) Si? A critical review on current approaches,” *Semicond. Sci. Technol.*, vol. 33, no. 9, p. 093002, Sep. 2018, doi: 10.1088/1361-6641/aad655.
- [21] K. Volz, W. Stolz, A. Dadgar and A. Krost, “Growth of III/Vs on Silicon,” in *Handbook of Crystal Growth*, Elsevier, 2015, pp. 1249–1300.
- [22] A. C. Lin, M. M. Fejer, and J. S. Harris, “Antiphase domain annihilation during growth of GaP on Si by molecular beam epitaxy,” *J. Cryst. Growth*, vol. 363, pp. 258–263, Jan. 2013, doi: 10.1016/j.jcrysgro.2012.10.055.
- [23] A. Beyer and K. Volz, “Advanced Electron Microscopy for III/V on Silicon Integration,” *Adv. Mater. Interfaces*, vol. 6, no. 12, p. 1801951, Jun. 2019, doi: 10.1002/admi.201801951.
- [24] S. Hosseini Vajargah, S. Y. Woo, S. Ghanad-Tavakoli, R. N. Kleiman, J. S. Preston, and G. A. Botton, “Atomic-resolution study of polarity reversal in GaSb grown on Si by

scanning transmission electron microscopy,” *J. Appl. Phys.*, vol. 112, no. 9, p. 093101, Nov. **2012**, doi: 10.1063/1.4759160.

[25] E. Tea, J. Vidal, L. Pedesseau, C. Cornet, J.-M. Jancu, J. Even, S. Laribi1, J.-F. Guillemoles and O. Durand, “Theoretical study of optical properties of anti-phase domains in GaP,” *J. Appl. Phys.*, vol. 115, no. 6, p. 063502, Feb. **2014**, doi: 10.1063/1.4864421

[26] Lipin Chen, Oliver Skibitzki, Laurent Pedesseau, Antoine Létoublon, Julie Stervinou, Rozenn Bernard, Christophe Levallois, Rozenn Piron, Mathieu Perrin, Markus Andreas Schubert, Alain Moréac, Olivier Durand, Thomas Schroeder, Nicolas Bertru, Jacky Even, Yoan Léger and Charles Cornet, “Strong Electron–Phonon Interaction in 2D Vertical Homovalent III–V Singularities,” *ACS Nano*, vol. 14, no. 10, pp. 13127–13136, Oct. **2020**, doi: 10.1021/acsnano.0c04702.

[27] B.Galiana, I.Rey-Stollec, I.Beinik, C.Algora, C.Teichert, J.M.Molina-Aldareguia and P.Tejedor, “Characterization of antiphase domains on GaAs grown on Ge substrates by conductive atomic force microscopy for photovoltaic applications,” *Sol. Energy Mater. Sol. Cells*, vol. 95, no. 7, pp. 1949–1954, Jul. **2011**, doi: 10.1016/j.solmat.2010.12.021.

[28] J. C. Norman, D. Jung, Y. Wan, and J. E. Bowers, “Perspective: The future of quantum dot photonic integrated circuits,” *APL Photonics*, vol. 3, no. 3, p. 030901, Mar. **2018**, doi: 10.1063/1.5021345.

[29] Rasool Saleem-Urothodi, Julie Le Pouliquen, Tony Rohel, Rozenn Bernard, Christelle Pareige, Alejandro Lorenzo-Ruiz, Alexandre Beck, Antoine Létoublon, Olivier De Sagazan, Charles Cornet, Yannick Dumeige and Yoan Léger, “Loss assessment in random crystal polarity gallium phosphide microdisks grown on silicon,” *Opt. Lett.*, vol. 45, no. 16, pp. 4646–4649, Aug. **2020**, doi: 10.1364/OL.399935.

[30] H. Kroemer, “Polar-on-nonpolar epitaxy,” *J. Cryst. Growth*, vol. 81, no. 1, pp. 193–204, Feb. **1987**, doi: 10.1016/0022-0248(87)90391-5.

- [31] D. J. Chadi, “Stabilities of single-layer and bilayer steps on Si(001) surfaces,” *Phys. Rev. Lett.*, vol. 59, no. 15, pp. 1691–1694, Oct. **1987**, doi: 10.1103/PhysRevLett.59.1691.
- [32] J. Dabrowski and H.-J. Mssig, “Silicon Surfaces and Formation of Interfaces: Basic Science in the Industrial World”. World Scientific, **2000**, <https://doi.org/10.1142/3615>.
- [33] B. Shi and K. M. Lau, “Chapter Seven - Growth of III–V semiconductors and lasers on silicon substrates by MOCVD,” in *Semiconductors and Semimetals*, vol. 101, S. Lourduoss, J. E. Bowers, and C. Jagadish, Eds. Elsevier, **2019**, pp. 229–282.
- [34] “About us - NAsP.” https://www.nasp.de/about_us.html (accessed May 18, **2020**).
- [35] C. S. C. Barrett *et al.*, “Effect of bulk growth temperature on antiphase domain boundary annihilation rate in MOCVD-grown GaAs on Si(001),” *J. Cryst. Growth*, vol. 450, pp. 39–44, Sep. **2016**, doi: 10.1016/j.jcrysgro.2016.06.021.
- [36] R. Alcotte, M. Martin, J. Moeyaert, R. Cipro, S. David, F. Bassani, F. Ducroquet, Y. Bogumilowicz, E. Sanchez, Z. Ye, X. Y. Bao, J. B. Pin, and T. Baron, “Epitaxial growth of antiphase boundary free GaAs layer on 300 mm Si(001) substrate by metalorganic chemical vapour deposition with high mobility,” *APL Mater.*, vol. 4, no. 4, p. 046101, Apr. **2016**, doi: 10.1063/1.4945586.
- [37] Qiang Li, Yating Wan, Alan Y. Liu, Arthur C. Gossard, John E. Bowers, Evelyn L. Hu, and Kei May Lau, “13- μm InAs quantum-dot micro-disk lasers on V-groove patterned and unpatterned (001) silicon,” *Opt. Express*, vol. 24, no. 18, p. 21038, Sep. **2016**, doi: 10.1364/OE.24.021038.
- [38] H. Schmid, M. Borg, K. Moselund, L. Gignac, C. M. Breslin, J. Bruley, D. Cutaia, and H. Riel, “Template-assisted selective epitaxy of III–V nanoscale devices for co-planar heterogeneous integration with Si,” *Appl. Phys. Lett.*, vol. 106, no. 23, p. 233101, Jun. **2015**, doi: 10.1063/1.4921962.

- [39] S. Mauthe, B. Mayer, M. Sousa, G. Villares, P. Staudinger, H. Schmid, K. Moselund, “Monolithically integrated InGaAs microdisk lasers on silicon using template-assisted selective epitaxy,” in *Nanophotonics VII*, May **2018**, vol. 10672, p. 106722U, doi: 10.1117/12.2306640.
- [40] Z. Yan, Y. Han, and K. M. Lau, “InAs nano-ridges and thin films grown on (001) silicon substrates,” *J. Appl. Phys.*, vol. 128, no. 3, p. 035302, Jul. **2020**, doi: 10.1063/5.0011808.
- [41] M. Kawabe and T. Ueda, “Self-Annihilation of Antiphase Boundary in GaAs on Si(100) Grown by Molecular Beam Epitaxy,” *Jpn. J. Appl. Phys.*, vol. 26, no. Part 2, No. 6, pp. L944–L946, Jun. **1987**, doi: 10.1143/JJAP.26.L944.
- [42] H. Noge, H. Kano, T. Kato, M. Hashimoto, and I. Igarashi, “Molecular beam epitaxial growth of a GaAs layer free from antiphase domains on an exactly (100)-oriented Si substrate preheated at 1000°C,” *J. Cryst. Growth*, vol. 83, no. 3, pp. 431–436, Jun. **1987**, doi: 10.1016/0022-0248(87)90306-X.
- [43] J. Varrio, H. Asonen, J. Lammasniemi, K. Rakennus, and M. Pessa, “Model of growth of single-domain GaAs layers on double-domain Si substrates by molecular beam epitaxy,” *Appl. Phys. Lett.*, vol. 55, no. 19, pp. 1987–1989, Nov. **1989**, doi: 10.1063/1.102141.
- [44] H. Kawanami, A. Hatayama, K. Nagai, and Y. Hayashi, “The Growth of Single Domain GaAs Films on Double Domain Si(001) Substrates by Molecular Beam Epitaxy,” *Jpn. J. Appl. Phys.*, vol. 26, no. Part 2, No. 3, pp. L173–L175, Mar. **1987**, doi: 10.1143/JJAP.26.L173.
- [45] P. R. Pukite and P. I. Cohen, “Multilayer step formation after As adsorption on Si (100): Nucleation of GaAs on vicinal Si,” *Appl. Phys. Lett.*, vol. 50, no. 24, pp. 1739–1741, Jun. **1987**, doi: 10.1063/1.97733.
- [46] A. Georgakilas, J. Stoemenos, K. Tsagaraki, Ph. Komninou, N. Flevaris, P. Panayotatos And A. Christou, “Generation and annihilation of antiphase domain boundaries in GaAs on Si grown by molecular beam epitaxy,” *J. Mater. Res.*, vol. 8, no. 08, Art. no. 08, Aug. **1993**, doi: 10.1557/JMR.1993.1908.

- [47] Marta Rio Calvo, Laura Monge Bartolomé, Michaël Bahriz, Guilhem Boissier, Laurent Cerutti, Jean-Baptiste Rodriguez, and Eric Tournié, “Mid-infrared laser diodes epitaxially grown on on-axis (001) silicon,” *Optica*, vol. 7, no. 4, p. 263, Apr. **2020**, doi: 10.1364/OPTICA.388383.
- [48] Keshuang Li, Junjie Yang, Ying Lu, Mingchu Tang, Pamela Jurczak, Zizhuo Liu, Xuezhe Yu, Jae-Seong Park, Huiwen Deng, Hui Jia, Manyu Dang, Ana M. Sanchez, Richard Beanland, Wei Li, Xiaodong Han, Jin-Chuan Zhang, Huan Wang, Fengqi Liu, Siming Chen, Alwyn Seeds, Peter Snowton, Huiyun Liu, “Inversion Boundary Annihilation in GaAs Monolithically Grown on On-Axis Silicon (001),” *Adv. Opt. Mater.*, vol. 8, no. 22, p. 2000970, Nov. **2020**, doi: 10.1002/adom.202000970.
- [49] C. Barrett, T. Martin, X.-Y. Bao, P. Martin, E. Sanchez, and K. s Jones, “Determination of Antiphase Domain Boundary Annihilation Rate in GaAs on Si(001) and the Influence of MOCVD Growth Temperature,” *ECS Trans.*, vol. 72, pp. 335–340, May **2016**, doi: 10.1149/07204.0335ecst.
- [50] O. Rubel and S. Baranovskii, “Formation Energies of Antiphase Boundaries in GaAs and GaP: An ab Initio Study,” *Int. J. Mol. Sci.*, vol. 10, no. 12, pp. 5104–5114, Nov. **2009**, doi: 10.3390/ijms10125104.
- [51] Y. Wang, “PhD Thesis: Structural analyses by advanced X-ray scattering on GaP layers epitaxially grown on silicon for integrated photonic applications,” **2016**.
- [52] I. Lucci, S. Charbonnier, L. Pedesseau, M. Vallet, L. Cerutti, J.-B. Rodriguez, E. Tournié, R. Bernard, A. Letoublon, N. Bertru, A. Le Corre, S. Rennesson, F. Semond, G. Patriarche, L. Largeau, P. Turban, A. Ponchet and C. Cornet, “Universal description of III-V/Si epitaxial growth processes,” *Phys. Rev. Mater.*, vol. 2, no. 6, Jun. **2018**, doi: 10.1103/PhysRevMaterials.2.060401.
- [53] C. Cornet, S. Charbonnier, I. Lucci, L. Chen, A. Létoublon, A. Alvarez, K. Tavernier, T. Rohel, R. Bernard, J.-B. Rodriguez, L. Cerutti, E. Tournié, Y. Léger, M. Bahri, G. Patriarche,

- L. Largeau, A. Ponchet, P. Turban, and N. Bertru, “Zinc-blende group III-V/group IV epitaxy: Importance of the miscut,” *Phys. Rev. Mater.*, vol. 4, no. 5, p. 053401, May **2020**, doi: 10.1103/PhysRevMaterials.4.053401.
- [54] R. M. Feenstra and J. A. Stroscio, “5.3. Gallium Arsenide,” in *Methods in Experimental Physics*, vol. 27, J. A. Stroscio and W. J. Kaiser, Eds. Academic Press, **1993**, pp. 251–276. doi: 10.1016/S0076-695X(08)60012-5.
- [55] T. Shitara, J. Zhang, J. H. Neave, and B. A. Joyce, “Ga adatom incorporation kinetics at steps on vicinal GaAs (001) surfaces during growth of GaAs by molecular beam epitaxy,” *J. Appl. Phys.*, vol. 71, no. 9, pp. 4299–4304, May **1992**, doi: 10.1063/1.350811.
- [56] T. Shitara, J. Zhang, J. H. Neave, and B. A. Joyce, “As/Ga ratio dependence of Ga adatom incorporation kinetics at steps on vicinal GaAs(001) surfaces,” *J. Cryst. Growth*, vol. 127, no. 1–4, pp. 494–498, Feb. **1993**, doi: 10.1016/0022-0248(93)90668-M.
- [57] M. Rio Calvo, J.-B. Rodriguez, L. Cerutti, M. Ramonda, G. Patriarche, and E. Tournié, “Molecular-beam epitaxy of GaSb on 6°-offcut (0 0 1) Si using a GaAs nucleation layer,” *J. Cryst. Growth*, vol. 529, p. 125299, Jan. **2020**, doi: 10.1016/j.jcrysgro.2019.125299.
- [58] P. Klapetek, D. Nečas, and C. Anderson, “Gwyddion user guide,” p. 217.
- [59] B. Arpapak, Y. E. Suyolcu, G. Çorapçioğlu, P. A. van Aken, M. A. Gülgün, and U. Serincan, “A comparative study on GaSb epilayers grown on nominal and vicinal Si(100) substrates by molecular beam epitaxy,” *Semicond. Sci. Technol.*, vol. 36, no. 2, p. 025011, Feb. **2020**, doi: 10.1088/1361-6641/abce1b.
- [60] A. Beyer, J. Ohlmann, S. Liebich, H. Heim, G. Witte, W. Stolz, and K. Volz, “GaP heteroepitaxy on Si(001): Correlation of Si-surface structure, GaP growth conditions, and Si-III/V interface structure,” *J. Appl. Phys.*, vol. 111, no. 8, p. 083534, Apr. **2012**, doi: 10.1063/1.4706573.

[61] B. Arpapay and U. Serincan, “The role of antiphase domain boundary density on the surface roughness of GaSb epilayers grown on Si (001) substrates,” *Superlattices Microstruct.*, vol. 140, p. 106450, Apr. **2020**, doi: 10.1016/j.spmi.2020.106450.

[62] Z. Loghmari, J.-B. Rodriguez, A. N. Baranov, M. Rio-Calvo, L. Cerutti, A. Meguekam, M. Bahriz, R. Teissier, and E. Tournié, “InAs-based quantum cascade lasers grown on on-axis (001) silicon substrate,” *APL Photonics*, vol. 5, no. 4, p. 041302, Apr. **2020**, doi: 10.1063/5.0002376.

Table of contents entry

The formation mechanism of anti-phase boundaries as well as the way they can self-annihilate has been debated for more than 30 years. It is experimentally demonstrated that the anti-phase domain is buried due to the phase-dependent growth rate introduced by a proper organization of the atomic steps at the Silicon surface.

Marta Rio Calvo, Jean-Baptiste Rodriguez*, Charles Cornet, Laurent Cerutti, Michel Ramonda, Achim Trampert, Gilles Patriarche and Éric Tournié*.

Crystal Phase Control During Epitaxial Hybridization of III-V Semiconductors with Silicon

Table of contents figure (55 mm broad x 50 mm high)

